

Hidden sector behind the CKM matrix

Shohei Okawa¹ and Yuji Omura²

¹ *Department of Physics, Nagoya University, Nagoya 464-8602, Japan*

² *Kobayashi-Maskawa Institute for the Origin of Particles and the Universe,
Nagoya University, Nagoya 464-8602, Japan*

Abstract

The small quark mixing, described by the Cabibbo-Kobayashi-Maskawa (CKM) matrix in the Standard Model, may be a clue to reveal new physics around the TeV scale. We consider a simple scenario that extra particles in a hidden sector radiatively mediate the flavor violation to the quark sector around the TeV scale and effectively realize the observed CKM matrix. The lightest particle in the hidden sector, whose contribution to the CKM matrix is expected to be dominant, is a good dark matter (DM) candidate. There are many possible setups to describe this scenario, so that we investigate some universal predictions of this kind of model, focusing on the contribution of DM to the quark mixing and flavor physics. In this scenario, there is an explicit relation between the CKM matrix and flavor violating couplings, such as four-quark couplings, because both are radiatively induced by the particles in the hidden sector. Then, we can explicitly find the DM mass region and the size of Yukawa couplings between the DM and quarks, based on the study of flavor physics and DM physics. In conclusion, we show that DM mass in our scenario is around the TeV scale, and the Yukawa couplings are between $\mathcal{O}(0.01)$ and $\mathcal{O}(1)$. The spin-independent DM scattering cross section is estimated as $\mathcal{O}(10^{-9})$ [pb]. An extra colored particle is also predicted at the $\mathcal{O}(10)$ TeV scale.

1 Introduction

The flavor structure of the Standard Model (SM) is one of mysteries, which are expected to be solved by extending the SM. In the SM, there are three generations in both quark and lepton sectors, and the difference among the generations is the size of the fermion masses. The fermion masses are dynamically generated by the spontaneous electroweak (EW) symmetry breaking, and the observed masses and mixing are given by the Yukawa couplings with the Higgs field in the SM. We know that the Yukawa couplings have to realize the large mass hierarchies and the small quark mixing. This unique form of the Yukawa matrix may be a clue to reveal the new physics above the EW scale.

If the Yukawa couplings are ignored in the SM Lagrangian, the flavor symmetry to rotate generations and phases of quarks is restored. Of these, the rotation symmetry of the generations is broken by quark mass terms; on the other hand, the symmetry to rotate the quark phases is respected even in the mass terms. The phase rotation is explicitly broken only by the Cabibbo-Kobayashi-Maskawa (CKM) matrix in the weak interaction. According to the experimental results, the CKM matrix is close to the 3×3 identity matrix but has small mixing angles. These small mixing angles may imply that the flavor symmetry, especially to rotate the quark phases, is respected at high energy. If this is the case, new physics exists above the EW scale in order to break the flavor symmetry spontaneously and generate the realistic quark mixing. This simple scenario, however, possibly suffers from constraints from flavor violating processes. If the flavor symmetry breaking of the Yukawa couplings is generated at the tree level, large flavor changing neutral currents (FCNCs) are generally induced and the model is easily excluded. Therefore, we need consider a scenario that some new particles mediate the flavor symmetry breaking to the quark sector at a loop level.

We have another strong motivation to desire new physics above the EW scale, that is, the results of the cosmological observations proposed by the WMAP and Planck collaborations [1,2]. They suggest that dark energy and dark matter (DM) dominate our universe and the amount of DM is about five times bigger than the visible particles. There are a lot possibilities for DM and one possible DM candidate is a Weakly-Interacting Massive Particle (WIMP) which resides around TeV scale. Then, we can expect that there is a direct connection between DM and the origin of the quark matrix.

Motivated by those mysteries, in this paper, we consider a simple scenario that extra particles, including DM, radiatively mediate the flavor symmetry breaking to the quark sector around the TeV scale and effectively realize the observed quark mixing. In our scenario, the flavor symmetry to rotate the quark phases in each generation is conserved at high energy in both of the up-type and down-type quark sectors. At the $\mathcal{O}(10)$ TeV scale, the flavor symmetry breaks down in a hidden sector. We also introduce an extra heavy quark and scalars charged under the flavor symmetry to mediate the flavor symmetry breaking to the quark sector. The mediators have flavor symmetric Yukawa couplings with only down-type quarks, but the fields to break the flavor symmetry do not couple to any SM fermions directly. The scalar mediators are only the fields to couple with the symmetry breaking fields, and then radiatively mediate the flavor symmetry breaking

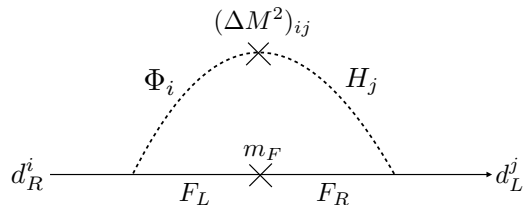


Figure 1: Rough sketch of our idea to generate the flavor violation. ΔM_{ij} breaks the flavor symmetry.

to the quark sector. We do not construct any explicit model for the flavor symmetry breaking, assuming that the effect of the symmetry breaking appears in the mass matrix of the scalar mediators. The rough sketch of this idea is shown in Fig. 1. Φ_i , H_i and F correspond to the SM-singlet, the EW charged scalars, and the extra heavy quark as the mediators. $(\Delta M)_{ij}$ is the part of the mass matrix for the scalars and denotes the flavor symmetry breaking effect. Note that we can find many similar setups motivated by the origin of the quark mixing [3–28]. In the present work, we consider a simple setup motivated by DM as well as the explanation of the quark mixing, and survey predictions of this kind of model. The results could be applied to many concrete models that radiatively induce the quark mixing.

The lightest neutral particle among the scalars, Φ_i and H_i , is a good DM candidate. The one-loop contribution to the down-type quark Yukawa couplings in Fig. 1 is probably dominated by the contribution of the diagram involving the DM, because of the relatively light mass. Then, we simply focus on the physics of the DM and estimate the size of the predicted quark mixing and quark masses. As mentioned above, there are many possible setups to describe this kind of scenario [3–28]. We could find some universal predictions, according to this simple assumption that the observed CKM matrix is originated from the one-loop corrections involving the DM.

Interestingly, the one-loop correction is roughly estimated as $\mathcal{O}(10^{-3})$ when the coupling between DM and quarks is a little smaller than $\mathcal{O}(1)$. It is close to the order of the strange quark mass divided by the vacuum expectation value (VEV) of the Higgs field. In order to realize the CKM matrix, the required correction to the down-type Yukawa matrix is also between $\mathcal{O}(10^{-6})$ and $\mathcal{O}(10^{-4})$, so that the couplings between DM and quarks should be in the range between $\mathcal{O}(0.01)$ and $\mathcal{O}(1)$, depending on the DM mass. Then, we need not worry about the triviality bound concerned with the divergence of couplings and we can predict a sizable interaction between DM and nuclei.

Another important prediction is a direct connection between the CKM matrix and flavor violating couplings, such as four-quark couplings. In this kind of setup, the CKM matrix and the flavor-violating couplings have the same source, so that sizable deviations from the SM values in the flavor violating processes are predicted. It is known that the $\Delta F = 2$ processes and the electric dipole moment (EDM) give stringent bounds to new physics contributions, so that the flavor physics constrains the mass scale of the heavy quark and the extra scalars. In our work, we see that the non-vanishing CP phases in the Wilson coefficients of the $\Delta S = 2$ and the EDM operators are unavoidable, and then we conclude that the extra quark mass should be not less than about 10 TeV. Taking into account the vacuum stability and the relic density of DM, the DM mass range is predicted to be between about 1 TeV and 10 TeV. We also find an explicit prediction of the spin-independent DM scattering cross section in Sec. 4: $\sigma_{\text{SI}} \simeq 1.7 \times 10^{-9}$ [pb]. Then, we conclude that our DM candidate can be tested by the future prospect of the XENON1T experiment [29].

In Sec. 2, we introduce our setup and explain the underlying theory of our scenario. Then, we discuss how to realize the observed Yukawa couplings in the SM. Since there are correlations between the predicted CKM matrix and the contributions to the flavor violating processes involving DM, we can explicitly derive the DM mass region. This study is given in Sec. 3. Based on the study in Sec. 3, we discuss the DM physics in Sec. 4. In the last section, we summarize our results and give a short comment on the other setup of the mediation and hidden sectors, motivated by the origin of the quark mass matrices.

2 Setup

We propose a scenario that the small quark mixing in the SM is originated from flavor symmetry breaking in a hidden sector. In our assumption, there is a flavor symmetry to rotate quark phases in each generation. The flavor symmetry is spontaneously broken by some fields in the hidden sector at some scale. The SM quarks do not directly couple with any fields to break the flavor symmetry, but there exist an extra quark and extra scalars to mediate the breaking effect to the quark sector. The fields to mediate the breaking effect do not contribute to the dynamics of the flavor symmetry breaking, but the masses and the mass eigenstates are affected by the symmetry breaking.

First, let us summarize the matter content of the quark sector. The fields in the flavor base are shown in Table 2. \hat{Q}_L^i , \hat{u}_R^i , and \hat{d}_R^i ($i = 1, 2, 3$) are the left-handed quarks, right-handed up-type and down-type quarks in the flavor base. We introduce a flavor symmetry to rotate the quark phases and assign a flavor charge (q_i) to each quark such that the flavor symmetry is conserved even in the Yukawa interaction with the Higgs doublet (H):

$$V_Y = y_i^u \overline{\hat{Q}_L^i} \tilde{H} \hat{u}_R^i + y_i^d \overline{\hat{Q}_L^i} H \hat{d}_R^i. \quad (1)$$

The Yukawa couplings, y_i^u and y_i^d , are in the diagonal forms, so that no quark flavor mixing appears at this level. Note that the flavor symmetry is not needed to be continuous

Fields	spin	SU(3) _c	SU(2) _L	U(1) _Y	flavor charge
\hat{Q}_L^i	1/2	3	2	1/6	q_i
\hat{u}_R^i	1/2	3	1	2/3	q_i
\hat{d}_R^i	1/2	3	1	-1/3	q_i
H	0	1	2	1/2	0

Table 1: SM particles with flavor charges.

symmetry, like U(1). It is not specified in our paper, assuming that the flavor symmetry is broken only in the hidden sector above the EW scale.

In the hidden sector there are extra fields to break the flavor symmetry and mediate the breaking effect. Let us introduce flavor-charged scalars, Φ_i and H_i , together with a flavor-singlet colored particle, F . The SM charges of F are the same as the ones of right-handed down-type quarks. Φ_i and H_i are SM-singlet complex scalar and SU(2)_L doublets charged under the flavor symmetry, respectively. Then, we write down the flavor conserving Yukawa couplings between the extra fields and down-type quarks:

$$V_{\text{extra}} = \hat{\lambda}_i \overline{F}_L \Phi_i^\dagger \hat{d}_R^i + \hat{\kappa}_i \overline{\hat{Q}}_L^i H_i F_R. \quad (2)$$

Here, we simply assume that the flavor symmetry is broken by some fields in the hidden sector except for Φ_i and H_i , and the mass eigenstates of Φ_i and H_i are fixed by the scalar potential involving the fields to break the symmetry.* Then, we rewrite the scalars in the flavor base with the mass eigenstates denoted by X , $\phi_{1,2}$, H_D , and $H'_{1,2}$:

$$\Phi_i = c_i^X X + c_i^{\phi_1} \phi_1 + c_i^{\phi_2} \phi_2, \quad H_i = c_i^D H_D + c_i^{H'_1} H'_1 + c_i^{H'_2} H'_2. \quad (3)$$

Each of the coefficients is given by the mass matrix including $(\Delta M)_{ij}$ in Fig. 1. All of the scalars radiatively contribute to the quark mixing through the Yukawa coupling in Eq. (2). The size of the contribution from each scalar would depend on the detail of models. In fact, we can consider many setups to realize the observed quark mass matrix radiatively in the framework of the Grand Unified Theory [3–6], Left-Right symmetric models [7–9], supersymmetric models [10–21], and flavor symmetric models [22–28]. Our main motivations are, however, to find the connection between DM and the quark mixing in the SM and to look for universal predictions of this kind of model. Therefore, we especially concentrate on the case that the light scalars dominantly contribute to the quark mixing, and the lightest scalar is a DM candidate. In particular, we focus on a

*The flavor symmetry might be explicitly broken. We do not specify the structure of the hidden sector. In the case that the flavor symmetry is spontaneously broken in the hidden sector, we can easily construct a model introducing extra flavored SM-singlet fields, φ_i . The potential for the flavor symmetry breaking is, for instance, given by $V_{SB} = -\mu_i^2 |\varphi_i|^2 + \lambda_i |\varphi_i|^4$, and each φ_i develops non-vanishing VEV. Note that φ_i could be real scalars, depending on the flavor symmetry.

minimal setup to realize the observed quark mass matrix; that is, there are only two kinds of light scalars, X and H_D , in our simplified model. Assuming that X and H_D are relatively lighter than the others, we can approximately simplify the Yukawa couplings as,

$$V_{\text{extra}}^{\text{app}} = \lambda_i \overline{F_L} X^\dagger \hat{d}_R^i + \kappa_i \overline{\hat{Q}_L^i} H_D F_R + \text{etc.} \quad (4)$$

We discuss the physics in our scenario, using these Yukawa couplings only: λ_i and κ_i . We will give some comments on the contributions of $\phi_{1,2}$ and $H'_{1,2}$. The charge assignment of the main fields for the mediation is summarized in Table 2. Note that dark charges are also assigned to F , H_D and X , to distinguish them from the SM particles. Thanks to the dark charge, X and/or the neutral component of H_D can be stable and good dark matter candidates to dominate our universe.

Fields	spin	SU(3) _c	SU(2) _L	U(1) _Y	Dark charge
F	1/2	3	1	-1/3	+1
H_D	0	1	2	1/2	-1
X	0	1	1	0	-1

Table 2: Extra particles in the mediation sector.

The scalar fields couple with the SM Higgs field as well, and the couplings, in addition to $V_{\text{extra}}^{\text{app}}$, are

$$\Delta V_{\text{extra}}^{\text{app}} = m_F \overline{F} F + A X H_D^\dagger H + m_X^2 |X|^2 + m_H^2 |H_D|^2. \quad (5)$$

Now, we expect that X and H_D do not develop non-vanishing VEVs because of the positive m_X^2 and m_H^2 . A is a trilinear coupling, that is effectively induced after the flavor symmetry breaking. The A term couples the SM Higgs and the mediators, so that plays an important role in generating the CKM matrix.

Note that the mass terms of X and H_D have a lower bound from the condition for the vacuum stability. If the trilinear coupling, A , is too large compared to m_X and m_H , unstable directions would appear at the origin. Then, we find the following condition for the mass terms:

$$m_X^2 m_H^2 > \frac{1}{2} A^2 v^2, \quad (6)$$

where v denotes the VEV of the Higgs field: $\langle H^T \rangle = (0, v/\sqrt{2})$.

2.1 Realization of the realistic Yukawa couplings

We discuss how the quark mixing is generated in our scenario. The Yukawa couplings at the tree-level are given by Eq. (1), so that they lead the diagonal mass matrices for

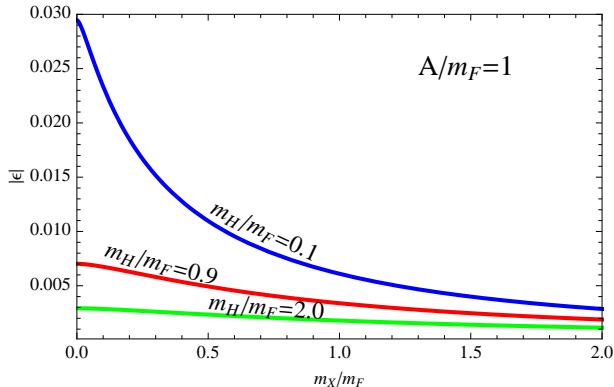


Figure 2: m_X/m_F vs. $|\epsilon|$ with $A/m_F = 1$ and $m_H/m_F = 0.1$ (blue), 0.9 (red), and 2.0 (green), respectively.

up-type and down-type quarks after the EW symmetry breaking:

$$(M_u)_{ij} = \frac{y_i^u}{\sqrt{2}} v \delta_{ij}, \quad (M_d^{(0)})_{ij} = \frac{y_i^d}{\sqrt{2}} v \delta_{ij}. \quad (7)$$

In our scenario, the flavor symmetry is broken in the hidden sector, and F , X and H_D decouple with the quark sector above the EW scale. Then, the small quark mixing is effectively generated via the Yukawa couplings in Eq. (4). According to the one-loop correction as shown in Fig. 1, we obtain the mass matrix for the down-type quarks in the form of

$$(M_d)_{ij} = (M_d^{(0)})_{ij} + \frac{v}{\sqrt{2}} \epsilon \kappa_i \lambda_j, \quad (8)$$

where ϵ is the factor that comes from the one-loop correction:

$$\epsilon = \frac{1}{16\pi^2} \frac{A}{m_F} \mathcal{Y}(m_H^2/m_F^2, m_X^2/m_F^2). \quad (9)$$

$\mathcal{Y}(x, y)$ is given by

$$\mathcal{Y}(x, y) = \frac{x(y-1) \ln x - y(x-1) \ln y}{(x-1)(x-y)(y-1)}. \quad (10)$$

m_F , m_X and m_H are the masses of the fields, F , X and H_D , respectively. A , m_X , and m_H are expected to be around the flavor symmetry breaking scale. The origin of m_F may be independent of the breaking scale. $|\epsilon|$ could be estimated as $\mathcal{O}(10^{-3})$ when A/m_F , m_X/m_F and m_H/m_F are larger than $\mathcal{O}(0.1)$. Fig. 2 shows m_X/m_F vs. $|\epsilon|$, assuming $m_H/m_F = 0.1$ (blue), 0.9 (red), 2.0 (green) and $A/m_F = 1$. We see that $|\epsilon|$ is expected to be between $\mathcal{O}(10^{-3})$ and $\mathcal{O}(10^{-2})$ in the parameter region. The required size of Yukawa couplings for the down-type quarks are less than $\mathcal{O}(10^{-2})$, so that the size of the loop correction can be compatible with the required values for the down-type quark masses, as well as the CKM matrix. Note that κ_i and λ_i are complex parameters, in principle, so CP phases are also generated by this dynamics.

Now, we define the mass eigenstates and derive the relation between the realistic mass matrix and the extra Yukawa couplings: κ_i and λ_i . The Yukawa matrix for the up-type quarks is in the diagonal form in Eq. (7). Precisely speaking, there would be additional contributions from the wave function renormalization factor and the loop correction involving $\phi_{1,2}$ and $H'_{1,2}$. The former is suppressed by y_i^d in the mass matrix and the later is assumed to be sub-dominant in our scenario.[†] Then, we approximately derive the following relation, using the mass matrix in Eq. (8):

$$(m_d)_i \delta_{ij} = \frac{v}{\sqrt{2}} \left\{ \left(V y^d V_R^\dagger \right)_{ij} + \epsilon (V \kappa)_i \left(\lambda V_R^\dagger \right)_j \right\}. \quad (11)$$

$(m_d)_i$ denote the quark masses: $(m_1^d, m_2^d, m_3^d) = (m_d, m_s, m_b)$. V is the CKM matrix and V_R is the diagonalizing matrix which rotates right-handed down-type quarks. Here, $V \kappa$ and λV_R^\dagger are the three-dimensional vectors, and they correspond to the Yukawa couplings with DM (scalars) and F in the mass base:

$$V_Y^{\text{ex}} = \left(\lambda V_R^\dagger \right)_i \overline{F}_L X^\dagger d_R^i + (V \kappa)_i \overline{d}_L^i H_D^0 F_R, \quad (12)$$

where d_L^i and d_R^i are the mass eigenstates. We define $\tilde{\kappa}_i \equiv V_{ij} \kappa_j$ and $\tilde{\lambda}_i = \lambda_j V_{R,ji}^\dagger$. In our notation, the mass eigenstates are $(d^1, d^2, d^3) = (d, s, b)$. As we see in Sec. 3, the flavor violating couplings that contribute to the $\Delta F = 2$ processes are also generated by the Yukawa couplings via the box diagram involving F , X and H_D . According to the relation in Eq. (11), $\tilde{\kappa}_i$ and $\tilde{\lambda}_i$ are explicitly related to the CKM matrix and the quark masses, so that we can expect to obtain explicit predictions to the flavor violating processes. Before the detailed analyses of the flavor physics, let us discuss the consistency with the realistic Yukawa couplings and estimate the size of $\tilde{\kappa}_i$ and $\tilde{\lambda}_i$ lead by Eq. (11).

Assuming $V_R \simeq V$ and using the relation of the diagonal elements in Eq. (11), y_i^d can be approximately estimated as

$$|y_1^d| = \mathcal{O}(\sqrt{2}m_d/v), \quad |y_2^d| = \mathcal{O}(\sqrt{2}m_s/v), \quad y_3^d \simeq \frac{\sqrt{2}}{v} m_b. \quad (13)$$

As discussed below, $\epsilon \tilde{\kappa}_2 \tilde{\lambda}_2$ becomes the same order as $\sqrt{2}m_s/v$, but $|y_2^d| = \mathcal{O}(\sqrt{2}m_s/v)$ is also required to be realistic.

Similarly, the off-diagonal elements of Eq. (11) lead the conditions for $\tilde{\kappa}_i$ and $\tilde{\lambda}_i$. The assumption, $V_R \simeq V$, implies $\tilde{\kappa}_i \tilde{\lambda}_j \simeq \tilde{\kappa}_j \tilde{\lambda}_i$ and each size is estimated as

$$|\tilde{\kappa}_1 \tilde{\lambda}_2| = \mathcal{O}(V_{us}), \quad |\tilde{\kappa}_1 \tilde{\lambda}_3| = \mathcal{O}(|V_{ub}| m_b/m_s), \quad |\tilde{\kappa}_2 \tilde{\lambda}_3| = \mathcal{O}(V_{cb} m_b/m_s). \quad (14)$$

Assuming $|\tilde{\kappa}_i| \simeq |\tilde{\lambda}_i|$, the alignment of $\tilde{\kappa}_i$ and $\tilde{\lambda}_i$ are expected to be

$$(|\tilde{\kappa}_1|, |\tilde{\kappa}_2|, |\tilde{\kappa}_3|) \simeq (|\tilde{\lambda}_1|, |\tilde{\lambda}_2|, |\tilde{\lambda}_3|) \simeq \left(\frac{|V_{ub}|}{|V_{cb}|}, 1, \frac{|V_{ub}|}{|V_{us}|} \frac{|y_3^d|}{|y_2^d|} \right) \times |\tilde{\lambda}_2|. \quad (15)$$

[†]Fig. 2 shows that we could obtain at least 10 % suppressions compared to the contributions of X and H_D , if the masses of $\phi_{1,2}$ and $H'_{1,2}$ are larger than m_F .

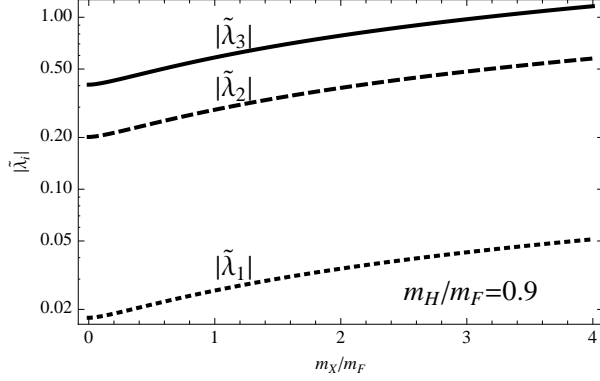


Figure 3: The Yukawa couplings, $\tilde{\lambda}_i$, depending on m_X/m_F . m_H/m_F and A/m_F are fixed at 0.9 and 1, respectively. $|\tilde{\kappa}_2| = |\tilde{\lambda}_2|$ and $|(V_R)_{ij}| = |V_{ij}|$ are assumed. Those assumptions lead $|\tilde{\lambda}_i| = |\tilde{\kappa}_i|$.

In our numerical study discussed below, we approximately evaluate $\tilde{\kappa}_i$ and $\tilde{\lambda}_j$, assuming

$$y_1^d = \frac{m_d\sqrt{2}}{v}, \quad y_3^d = \frac{m_b\sqrt{2}}{v}. \quad (16)$$

y_2^d is fixed by the (2, 2) element of Eq. (11). The off-diagonal elements of Eq. (11) lead $\tilde{\kappa}_i\tilde{\lambda}_j$: to a good approximation,

$$\begin{aligned} \tilde{\kappa}_1\tilde{\lambda}_2 &= -\frac{y_2^d}{\epsilon}V_{us}, \quad \tilde{\kappa}_2\tilde{\lambda}_1 = -\frac{y_2^d}{\epsilon}|(V_R)_{12}|e^{-i(\delta_R)_{12}}, \\ \tilde{\kappa}_1\tilde{\lambda}_3 &= -\frac{y_3^d}{\epsilon}V_{ub}, \quad \tilde{\kappa}_3\tilde{\lambda}_1 = -\frac{y_3^d}{\epsilon}|(V_R)_{13}|e^{-i(\delta_R)_{12}-i(\delta_R)_{23}-i\beta}, \\ \tilde{\kappa}_2\tilde{\lambda}_3 &= -\frac{y_3^d}{\epsilon}V_{cb}, \quad \tilde{\kappa}_3\tilde{\lambda}_2 = -\frac{y_3^d}{\epsilon}|(V_R)_{23}|e^{-i(\delta_R)_{23}}. \end{aligned} \quad (17)$$

β is from the CKM matrix: $V_{ub} = |V_{ub}|e^{-i\beta}$. Note that there is a prediction for V_R and y_i^d according to the mass matrix in Eq. (8):

$$\frac{Y_{31}}{Y_{13}} = \frac{Y_{21}Y_{32}}{Y_{12}Y_{23}} \quad (18)$$

where $Y_{ij} = \left(Vy^dV_R^\dagger\right)_{ij}$ is defined. $(V_R)_{ij}$ need satisfy this condition and $|(V_R)_{ij}| = |V_{ij}|$ is assumed in our study. Note that in this parametrization y_2^d is evaluated as

$$y_2^d = \frac{m_s\sqrt{2}}{v} \frac{V_{ub}}{V_{ub} - V_{us}V_{cb}}. \quad (19)$$

This estimation is a good approximation to realize the observed Yukawa couplings. We expect that there are also some corrections from other extra particles, such as $\phi_{1,2}$

$m_d(2 \text{ GeV})$	$4.8^{+0.5}_{-0.3} \text{ MeV}$ [30]	λ	$0.22509^{+0.00029}_{-0.00028}$ [31]
$m_s(2 \text{ GeV})$	$95 \pm 5 \text{ MeV}$ [30]	A	$0.8250^{+0.0071}_{-0.0111}$ [31]
$m_b(m_b)$	$4.18 \pm 0.03 \text{ GeV}$ [30]	$\bar{\rho}$	$0.1598^{+0.0076}_{-0.0072}$ [31]
$\frac{2m_s}{(m_u+m_d)}(2 \text{ GeV})$	27.5 ± 1.0 [30]	$\bar{\eta}$	$0.3499^{+0.0063}_{-0.0061}$ [31]
$m_c(m_c)$	$1.275 \pm 0.025 \text{ GeV}$ [30]	M_Z	$91.1876(21) \text{ GeV}$ [30]
$m_t(m_t)$	$160^{+5}_{-4} \text{ GeV}$ [30]	M_W	$80.385(15) \text{ GeV}$ [30]
α	$1/137.036$ [30]	G_F	$1.1663787(6) \times 10^{-5} \text{ GeV}^{-2}$ [30]
$\alpha_s(M_Z)$	$0.1193(16)$ [30]		

Table 3: The input parameters in our analysis. The CKM matrix, V , is written in terms of λ , A , $\bar{\rho}$ and $\bar{\eta}$ [30].

and $H'_{1,2}$, so we allow 10 % deviation in the down-type quark masses. In our analysis, we use the input parameters for the quark masses [30] and the CKM matrix [31] derived from the values in Table 3. When we compare our prediction with the realistic Yukawa couplings, we evaluate the quark masses at 1 TeV, using the SM RG running at the two-loop level [32, 33].

Figure 3 shows the size of $|\tilde{\lambda}_i|$ depending on m_X/m_F , assuming that $|\tilde{\kappa}_2| = |\tilde{\lambda}_2|$ and $|(V_R)_{ij}| = |V_{ij}|$. The CP phases and m_H/m_F are fixed at $(\delta_R)_{12} = (\delta_R)_{23} = 0$ and $m_H/m_F = 0.9$, respectively. It is interesting that this hierarchical Yukawa couplings, $\tilde{\lambda}_i$, have been proposed in Ref. [34], motivated by DM physics and flavor physics.

In Sec. 3, we discuss flavor physics in this setup and specify the DM mass region consistent with the experimental results. We see that $\tilde{\kappa}_i \tilde{\lambda}_j$, which appear in Eq. (11), directly relate to the flavor violating couplings which contribute to the $\Delta F = 2$ processes. Therefore, we can explicitly derive the lower bound on the flavor symmetry breaking scale.

3 Flavor physics

In this section, we discuss flavor physics in our scenario. As well known, the $\Delta F = 2$ processes, such as $K_0\text{-}\bar{K}_0$, are the most sensitive to the new physics contributions. In addition, the CP-violation and the rare meson decay possibly constrain our model. First, we study the $\Delta F = 2$ processes and discuss the deviations from the SM predictions, based on the result in Sec. 2. Then, we study the other observables: e.g., $B \rightarrow X_s \gamma$ and the neutron EDM. In particular, we see that our model is strongly constrained by the CP-violation of the $K_0\text{-}\bar{K}_0$ mixing and the EDM.

m_K	497.611(13) MeV [30]	m_{B_s}	5.3663(6) GeV [30]
F_K	155.8(17) MeV [35]	m_B	5.2795(3) GeV [30]
\hat{B}_K	0.7625(97) [36]	$f_{B_s}\sqrt{\hat{B}_{B_s}}$	270(16) MeV [36]
$(\Delta M_K)_{\text{exp}}$	$3.484(6)\times 10^{-12}$ MeV [30]	$f_B\sqrt{\hat{B}_B}$	219(14) MeV [36]
$ \epsilon_K _{\text{exp}}$	$2.228(11)\times 10^{-3}$ [30]	\hat{B}_{B_s}	1.32(6) [36]
η_1	1.87(76) [37]	\hat{B}_B	1.26(9) [36]
η_2	0.5765(65) [38]	η_B	0.55 [38]
η_3	0.496(47) [39]	η_Y	1.012 [40]

Table 4: The input parameters relevant to the $\Delta F = 2$ processes.

3.1 $\Delta F = 2$ processes

In our scenario, the CKM matrix is radiatively generated by F , X and H_D in the hidden sector. In addition, the extra fields induce the operators relevant to the $\Delta F = 2$ processes:

$$\begin{aligned} \mathcal{H}_{eff}^{\Delta F=2} = & (C_1)_{ij}(\bar{d}_L^i\gamma^\mu d_L^j)(\bar{d}_L^i\gamma_\mu d_L^j) + (\tilde{C}_1)_{ij}(\bar{d}_R^i\gamma^\mu d_R^j)(\bar{d}_R^i\gamma_\mu d_R^j) \\ & + (C_4)_{ij}(\bar{d}_L^i d_R^j)(\bar{d}_R^i d_L^j) + h.c.. \end{aligned} \quad (20)$$

The Wilson coefficients at the one-loop level are given by,

$$(C_1)_{ij} = \frac{(\tilde{\kappa}_i\tilde{\kappa}_j^*)^2}{64\pi^2 m_F^2} \mathcal{B}_1(m_H^2/m_F^2), \quad (21)$$

$$(\tilde{C}_1)_{ij} = \frac{(\tilde{\lambda}_i^*\tilde{\lambda}_j)^2}{64\pi^2 m_F^2} \mathcal{B}_1(m_X^2/m_F^2), \quad (22)$$

$$(C_4)_{ij} = -\frac{\tilde{\kappa}_i\tilde{\lambda}_j\tilde{\kappa}_j^*\tilde{\lambda}_i^*}{16\pi^2 m_F^2} \mathcal{B}(m_H^2/m_F^2, m_X^2/m_F^2), \quad (23)$$

where $\mathcal{B}_1(x, y)$ and $\mathcal{B}(x, y)$ are defined as

$$\mathcal{B}_1(x) = \frac{1}{(1-x)^2} \left(\frac{1+x}{2} + \frac{x}{1-x} \ln x \right), \quad (24)$$

$$\mathcal{B}(x, y) = \frac{-x(y-1)^2 \ln x + y(x-1)^2 \ln y - (x-1)(y-1)(x-y)}{(x-1)^2(y-1)^2(x-y)}. \quad (25)$$

As shown in Fig. 3, the Yukawa couplings, $\tilde{\kappa}_i$ and $\tilde{\lambda}_i$, are sizable in our models, so that the constraints from the $K_0\text{-}\bar{K}_0$ mixing should be taken into account, because it is the most sensitive to new physics among the observables of the $\Delta F = 2$ processes.

In the K system, we concentrate on ϵ_K and ΔM_K . They are approximately evaluated as

$$\epsilon_K = \frac{\kappa_\epsilon e^{i\varphi_\epsilon}}{\sqrt{2}(\Delta M_K)_{\text{exp}}} \text{Im}(M_{12}^K), \quad \Delta M_K = 2\text{Re}(M_{12}^K), \quad (26)$$

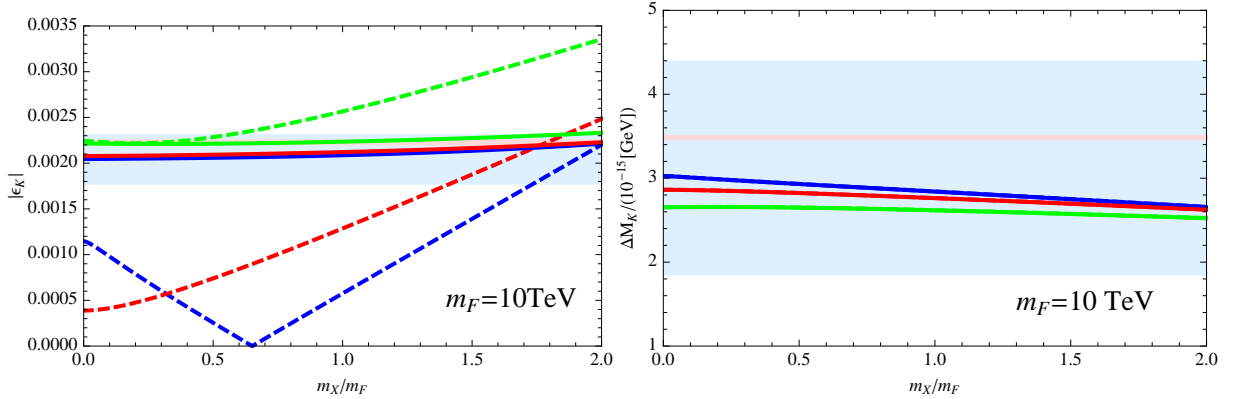


Figure 4: m_X/m_F vs. $|\epsilon_K|$ (left panel) and ΔM_K (right panel). m_F is fixed at $m_F = 10$ TeV. Each line corresponds to $m_H/m_F = 0.1$ (blue), 0.9 (red), and 2 (green). The phases of $(V_R)_{ij}$ are fixed at $(\delta_R)_{23} = 0$, $(\delta_R)_{12} = 0$ (thick line) and 0.1 (dashed line). The light blue band is the SM prediction with 1σ errors of $\eta_{1,2,3}$. The pink band corresponds to $|\epsilon_K|_{\text{exp}}$.

where κ_ϵ and φ_ϵ are $\kappa_\epsilon = 0.94 \pm 0.02$ and $\varphi_\epsilon = 0.2417 \times \pi$. $(\Delta M_K)_{\text{exp}}$ is the experimental value and M_{12}^K includes both the SM contribution and our prediction:

$$M_{12}^{K*} = (M_{12}^K)_{\text{SM}}^* + \left\{ (C_1)_{sd} + (\tilde{C}_1)_{sd} \right\} \times \frac{1}{3} m_K F_K^2 \hat{B}_K + (C_4)_{sd} \times \frac{1}{4} \left(\frac{m_K}{m_s + m_d} \right)^2 m_K F_K^2 B_4. \quad (27)$$

The first term is the SM prediction described by $(M_{12}^K)_{\text{SM}}$,

$$(M_{12}^K)_{\text{SM}}^* = \frac{G_F^2}{12\pi^2} F_K^2 \hat{B}_K m_K M_W^2 \left\{ V_c^2 \eta_1 S_0(x_c) + V_t^2 \eta_2 S_0(x_t) + 2V_c V_t \eta_3 S(x_c, x_t) \right\}, \quad (28)$$

where x_i and V_i denote $(m_i^u)^2/M_W^2$ and $V_{is}^* V_{id}$, respectively. $\eta_{1,2,3}$ correspond to the NLO and NNLO QCD corrections. The values of our input parameters are summarized in Table 4. In our numerical analysis of the predictions, we use the central values. Note that the central values of the input parameters for the CKM matrix give $|V_{cb}| = 41.80 \times 10^{-3}$ and $|V_{ub}| = 3.71 \times 10^{-3}$. For these matrix elements, it is known that there are discrepancies between the values derived from the exclusive and inclusive B decay. Each value is close to $|V_{cb}|$ ($|V_{ub}|$) of the inclusive (exclusive) decay, respectively. B_K and B_4 are the bag parameters that are derived from the lattice calculation [41]. Of interest is to note that the $(C_4)_{sd}$ contribution, which directly relates to the Yukawa couplings of the down-type quarks in Eq. (8), dominates over the other contributions. To evaluate the Wilson coefficient, $(C_4)_{ij}$, at $\mathcal{O}(1)$ GeV, we include the renormalization group (RG) correction at the one-loop level.

Setting $m_F = 10$ TeV and $m_H/m_F = 0.1$ (blue), 0.9 (red), 2 (green), we draw our predictions of $|\epsilon_K|$ (left panel) and ΔM_K (right panel) in Fig. 4. The new phases in $(V_R)_{ij}$

are fixed at $(\delta_R)_{23} = 0$, $(\delta_R)_{12} = 0$ (thick line) and 0.1 (dashed line), respectively. Using the central values in Table 4, $|\epsilon_K|$ of the SM prediction is estimated as $|\epsilon_K|_{\text{SM}} = 2.04 \times 10^{-3}$, that is slightly smaller than the experimental result: $|\epsilon_K|_{\text{exp}} = 2.228(11) \times 10^{-3}$ [30]. The SM prediction, however, suffers from the large uncertainty, so that it may be difficult to draw the explicit exclusion limit. As we see Table 4, the contributions involving charm quark has large errors, so that more than 10 % ambiguity still exists even in $|\epsilon_K|$ of the SM prediction. The light blue bands on both panels are the SM predictions with 1σ errors of $\eta_{1,2,3}$. The pink bands correspond to $|\epsilon_K|_{\text{exp}}$ and $|\Delta M_K|_{\text{exp}}$, respectively.

If we require the deviation of $|\epsilon_K|$ from the SM prediction to be within the error, there is an allowed parameter region in the $m_F = 10$ TeV case. The CP phase, $(\delta_R)_{12}$, is relevant to $|\epsilon_K|$, so that vanishing $(\delta_R)_{12}$ can evade the strong bound from the observable. As shown in Fig. 4, $|(\delta_R)_{12}|$ should be smaller than 0.1, unless m_H is larger than m_F .

In Fig. 5, we draw the region that the deviation of $|\epsilon_K|$ from the SM prediction is within the error of the SM prediction: $1.79 \times 10^{-3} \leq |\epsilon_K| \leq 2.30 \times 10^{-3}$. $(\delta_R)_{12}$, $(\delta_R)_{23}$ and A/m_F are fixed at $((\delta_R)_{12}, (\delta_R)_{23}, A/m_F) = (0.1, 0, 1)$. In the pink (cyan) region, the deviation is within the error in the case with $m_F = 20$ TeV (25 TeV). The exclusion limit reaches the dashed cyan line, when $m_F = 30$ TeV. The (light) gray region in Fig. 5 is excluded by the vacuum stability in Eq. (6) when $m_F = 20$ TeV (25 TeV) is satisfied.

H_D or X is a DM candidate, so that this figure shows the DM mass region, depending on m_F . For instance, both of H_D and X are lighter than F , when m_F is below 25 TeV. On the other hand, either H_D or X could be heavier than F , if m_F is 30 TeV or heavier. Note that the constraint from $|\epsilon_K|$ is drastically relaxed, when m_F is larger than 100 TeV.

In the same manner, we can evaluate the B_d - \bar{B}_d and B_s - \bar{B}_s mixing. The mass differences of the B mesons in our model are given by

$$\Delta M_{B_q} = 2 \left| M_{12}^{B_q} \right|^2 = 2 \left| (M_{12}^{B_q})_{\text{SM}} + \Delta M_{12}^{B_q} \right|^2 \quad (q = d, s). \quad (29)$$

$\Delta M_{12}^{B_q}$ describes the contributions of $(C_1)_{bq}$, $(\tilde{C}_1)_{bq}$ and $(C_4)_{bq}$ in Eq. (20). Figure 6 shows the deviations of ΔM_{B_d} (left panel) and ΔM_{B_s} (right panel), when m_F is fixed at 10 TeV. The parameter choice is the same as in Fig. 4. $\delta(\Delta M_{B_q}) = \Delta M_{B_q}/(\Delta M_{B_q})_{\text{SM}} - 1$ are defined in Fig. 6.

Using the central values in Table 4, ΔM_{B_d} and ΔM_{B_s} of the SM predictions are estimated as $\Delta M_{B_d} = 0.517$ [ps $^{-1}$] and $\Delta M_{B_s} = 18.358$ [ps $^{-1}$]. The experimental results are $\Delta M_{B_d} = 0.554_{-0.028}^{+0.035}$ [ps $^{-1}$] and $\Delta M_{B_s} = 16.89_{-0.35}^{+0.47}$ [ps $^{-1}$] [31], respectively. In this sense, $\delta(\Delta M_{B_d})$ should be positive and $\delta(\Delta M_{B_s})$ should be negative, although the errors of $f_{B_q} \sqrt{\hat{B}_{B_q}}$ in Table 4 cause about 10 % uncertainties for the SM predictions.

We see that the deviations are less than 1 % in ΔM_{B_q} . There is a small dependence of $(\delta_R)_{12}$ in ΔM_{B_d} , but the predicted deviation is not so large as far as m_F is larger than 10 TeV. In ΔM_{B_s} , the deviation is relatively large, compared to $\delta(\Delta M_{B_d})$. This is because $|\tilde{\lambda}_2|$ is about 10 times larger than $|\tilde{\lambda}_1|$. Depending on the scalar masses, $|\delta(\Delta M_{B_s})|$ could reach $\mathcal{O}(0.01)$.

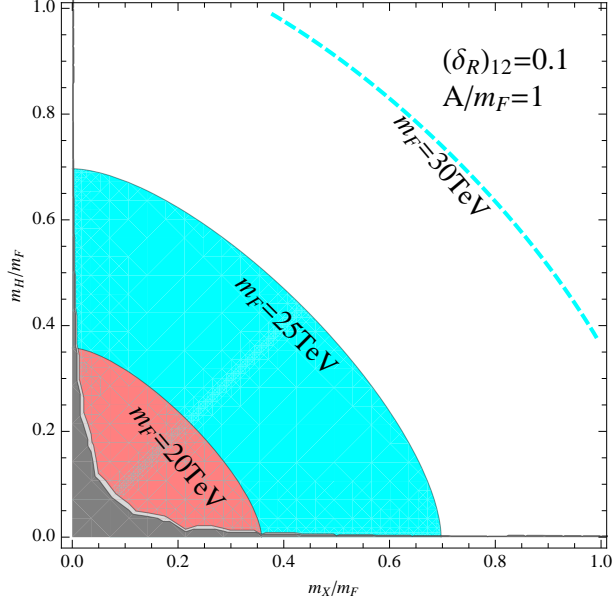


Figure 5: The region that $|\epsilon_K|$ is within $1.79 \times 10^{-3} \leq |\epsilon_K| \leq 2.30 \times 10^{-3}$ in the cases with $m_F = 20$ TeV (pink) and 25 TeV (cyan). $(\delta_R)_{12}$, $(\delta_R)_{23}$ and A/m_F are fixed at $((\delta_R)_{12}, (\delta_R)_{23}, A/m_F) = (0.1, 0, 1)$. The dashed cyan line corresponds to the exclusion limit of $m_F = 30$ TeV case. The (light) gray region is excluded by the vacuum stability when $m_F=20$ TeV (25 TeV) and $A/m_F = 1$ are satisfied.

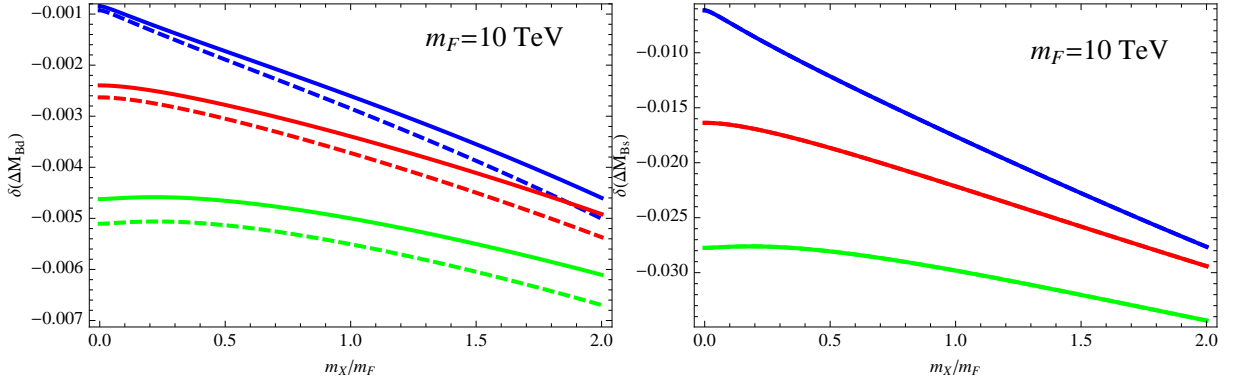


Figure 6: The deviations of ΔM_{B_d} and ΔM_{B_s} with $m_F = 10$ TeV. Each line corresponds to $m_H/m_F = 0.1$ (blue), 0.9 (red), and 2 (green). The phases of $(V_R)_{ij}$ are fixed at $(\delta_R)_{23} = 0$, $(\delta_R)_{12} = 0$ (thick line) and 0.1 (dashed line).

3.2 $B \rightarrow X_s \gamma$ and EDM

We have seen that the strongest constraint on our model is from $|\epsilon_K|$. In addition, we can find other flavor violating and CP-violating processes relevant to our scenario.

For instance, it is known that the rare B meson decay, $B \rightarrow X_s \gamma$, strongly constrains new physics contribution. In our scenario, the one-loop diagram involving the mediators contributes to the process. The effective operators are given by

$$\mathcal{H}_{eff}^{b \rightarrow s \gamma} = -g_{\text{SM}} \{C_7(\bar{s}_L \sigma^{\mu\nu} b_R)F_{\mu\nu} + C'_7(\bar{s}_R \sigma^{\mu\nu} b_L)F_{\mu\nu}\}, \quad (30)$$

where g_{SM} is defined as

$$g_{\text{SM}} = \frac{4G_F}{\sqrt{2}}(V_{ts}^* V_{tb}) \times \frac{e m_b}{16\pi^2}. \quad (31)$$

In our model, C_7 and C'_7 are predicted as

$$C_7 = \frac{g'}{g_{\text{SM}}} \frac{\tilde{\kappa}_2 \tilde{\lambda}_3}{96\pi^2 m_F^3} A \frac{v}{\sqrt{2}} \mathcal{B}(m_H^2/m_F^2, m_X^2/m_F^2), \quad (32)$$

$$C'_7 = \frac{g'}{g_{\text{SM}}} \frac{\tilde{\kappa}_3^* \tilde{\lambda}_2^*}{96\pi^2 m_F^3} A^* \frac{v}{\sqrt{2}} \mathcal{B}(m_X^2/m_F^2, m_H^2/m_F^2), \quad (33)$$

where g' is the gauge coupling of $U(1)_Y$. $|\epsilon_K|$ requires at least $\mathcal{O}(10)$ -TeV colored particle, so that C_7 and C'_7 are suppressed by v/m_F^2 . Fixing $m_F = 10$ TeV, we estimate those coefficients as $C_7 \simeq \mathcal{O}(10^{-3})$. Such a small parameter predicts at most a few % deviation of $\text{Br}(B \rightarrow X_s \gamma)$, so that we conclude that the branching ratio including the new physics contribution is consistent with the combined experimental result: $\text{Br}(B \rightarrow X_s \gamma) = (3.43 \pm 0.22) \times 10^{-4}$ [43].

The penguin diagrams also arise and contribute to $\Delta F = 1$ processes. In our model, those contributions are, however, suppressed by $(Av/m_X^2)^2$ or $(Av/m_H^2)^2$, that correspond to the mixing between X and H_D . Then, we can not expect large deviations in $\Delta F = 1$ processes through the penguin diagrams.

Finally, we discuss electric dipole moments (EDMs) in our model. $\tilde{\kappa}_i$ and $\tilde{\lambda}_i$, in general, have non-vanishing imaginary parts, because of the CP-violating phases of the CKM matrix and $(V_R)_{ij}$. The important point is that the relation in Eq. (11) limits the phase, as shown in Eq. (17). Then, we find that there is no parameter choice such that the CP-violating phases contributing to ϵ_K and EDMs cancel out at the same time. We plot our prediction of the neutron EDM, d_n , that is constrained as $|d_n| < 3.6 \times 10^{-26}$ [e cm] [42]. A lot of efforts have been done to improve the theoretical prediction [44–46]. We adopt the value in Ref. [46] and draw our prediction in Fig. 7. m_F is fixed at $m_F = 10$ TeV. Each line corresponds to $m_H/m_F = 0.1$ (blue), 0.9 (red), and 2 (green). The phases of $(V_R)_{ij}$ are fixed at $(\delta_R)_{23} = 0$, $(\delta_R)_{12} = 0$ (thick line) and 0.1 (dashed line), respectively. The dashed black line corresponds to the current exclusion limit: $|d_n| < 3.6 \times 10^{-26}$ [e cm] [42]. Our predictions are below the current experimental bound. Note that our prediction for $|d_n|$ becomes smaller when $(\delta_R)_{12}$ is about 0.45; on the other hand, $|\epsilon_K|$ becomes larger than in the $(\delta_R)_{12} \simeq 0$ case.

The measurement of the permanent EDM of neutral ^{199}Hg atom is developed and the current upper bound reaches $|d_{H_g}| < 7.4 \times 10^{-30}$ [e cm] [47]. This measurement, however, suffers from the large uncertainty of the theoretical prediction [46], so that it

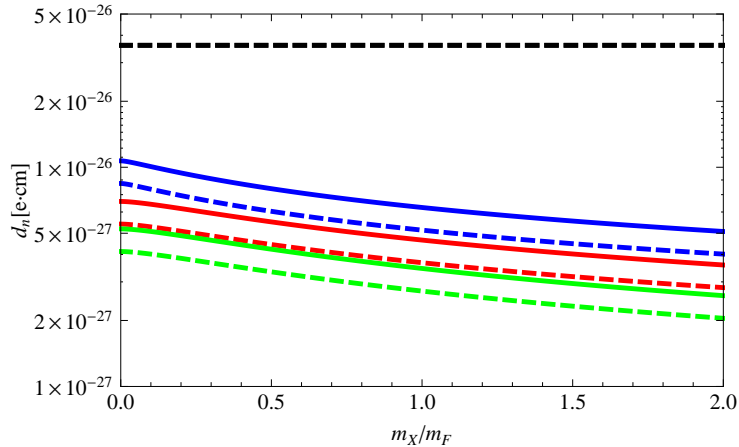


Figure 7: The neutron EDM with $m_F = 10$ TeV. Each line corresponds to $m_H/m_F = 0.1$ (blue), 0.9 (red), 2 (green). The phases of $(V_R)_{ij}$ are fixed at $(\delta_R)_{23} = 0$, $(\delta_R)_{12} = 0$ (thick line) and 0.1 (dashed line). The dashed black line corresponds to the current exclusion line: $|d_n| < 3.6 \times 10^{-26}$ [e cm] [42].

is still difficult to compare our prediction with the experimental bound. If we use the central values introduced in Ref. [47], our prediction estimated as $\mathcal{O}(10^{-29})$ [e cm] when $m_F = 10$ TeV, so that our model could be tested if the theoretical error is shrunken.

4 Dark matter physics

We have obtained the mass spectrum of the extra particles and the couplings between the extra particles and quarks, according to the realistic quark mass matrix and the flavor physics. Finally, we discuss DM physics in this section.

The DM candidate in our model is either X or the neutral component of H_D ,[‡] and both have couplings with the SM Higgs in the scalar potential as,

$$\lambda_X |X|^2 |H|^2 + \lambda_3 |H_D|^2 |H|^2 + \lambda_4 |H_D^\dagger H|^2, \quad (34)$$

in addition to the trilinear coupling, $A X H_D^\dagger H$, and the Yukawa couplings with down-type quarks. This type of DM has been studied recently [34]. The authors of Ref. [34] concentrate on the relatively light F case, and do the integrated research of the LHC physics, the flavor physics, and the DM physics. In our scenario, F should be at least $\mathcal{O}(10)$ TeV, to avoid too large deviations in the K_0 - \bar{K}_0 mixing and the EDM, so that our parameters are out of the region analyzed in Ref. [34].

When m_F is $\mathcal{O}(10)$ TeV and A/m_F is set to unit, the condition for the vacuum stability in Eq. (6) leads the DM mass region as

$$\frac{m_X m_H}{m_F^2} \gtrsim \mathcal{O}(10^{-2}). \quad (35)$$

[‡]We do not consider the case that both X and the neutral component of H_D are stable.

If we assume that there is no large hierarchy between m_X and m_H , this inequality means m_X and m_H should be not less than $\mathcal{O}(1)$ TeV.

The DM is thermally produced by the interactions with the SM Higgs in Eq. (34) and the Yukawa interactions with the down-type quarks and F . As shown in Fig. 3, the alignment of the Yukawa couplings is hierarchical, so that the annihilation of the DM to the bottom quarks is relatively larger in the t -channel F exchanging processes. The heavy F mass of $\mathcal{O}(10)$ -TeV, however, suppresses the annihilation, so that the main annihilation process is given by the interaction with the SM Higgs in Eq. (34). In order to achieve the observed relic abundance of DM, DM mass should be less than $\mathcal{O}(10)$ TeV, to respect the perturbativity of λ_X [48].[§] Assuming that X is DM, m_X should be in the range,

$$\mathcal{O}(1) \text{ TeV} \lesssim m_X \lesssim 10 \text{ TeV}. \quad (36)$$

The upper bound comes from $\lambda_X \leq \sqrt{4\pi}$ and the lower bound corresponds to Eq. (35). In this region, we can estimate the cross section for the direct detection. The dominant process is the SM Higgs exchanging, and the cross section is almost fixed once λ_X is given by the thermal relic density. The prediction of the spin-independent (SI) cross section with the nucleon at the direct detection experiments is

$$\sigma_{\text{SI}} \simeq 1.7 \times 10^{-9} \text{ [pb]}. \quad (37)$$

This prediction slightly depends on the DM mass, but the change is only a few percent as far as m_X is within the mass region in Eq. (36). Note that there is a small correction from the F exchanging in the SI cross section, Eq.(37), but we find that it is not more than 10% of the Higgs exchanging contribution when m_F is $\mathcal{O}(10)$ TeV. The current upper bound is given by the LUX and the PandaX-II experiments: $\sigma_{\text{SI}} \lesssim \mathcal{O}(10^{-8})$ [pb] [50–52]. In the future, the XENON1T experiment could reach $\mathcal{O}(10^{-9})$ pb [29], so that our scenario is expected to be probed by the direct detection of DM.

In the case that the neutral component of H_D is DM, the DM physics is more complicated because the DM interacts with the SM particles via the Z and W gauge boson exchanging. There are CP-even and CP-odd neutral scalars, and a charged scalar in H_D . The λ_4 term in the scalar potential generates the mass difference between the charged and neutral scalars, while this term does not split two neutral scalars. However, if the CP-even and the CP-odd scalars of H_D are degenerate, the Z -boson exchanging contribution dominates the cross section with the nuclei and the predicted σ_{SI} is excluded by the current experimental bound [48]. Therefore, the mass difference of two neutral scalars needs to be generated in this case. The mass splitting of the neutral scalars appears only when $\lambda_5(H_D^\dagger H)^2$ is allowed in the potential. If the dark symmetry is (global) $U(1)$, the λ_5 term is forbidden, so that we conclude the dark symmetry should be a discrete Z_2 symmetry when we discuss the case that the neutral component of H_D is DM.

In the annihilation processes, H_D can annihilate to Z and W gauge bosons as well as the SM fermions. When the DM mass region of H_D is not less than $\mathcal{O}(1)$ TeV, the

[§]Note that we can also derive the upper bound of DM mass from the unitarity of the annihilation cross section; that is, the upper bound is $\mathcal{O}(100)$ TeV [49].

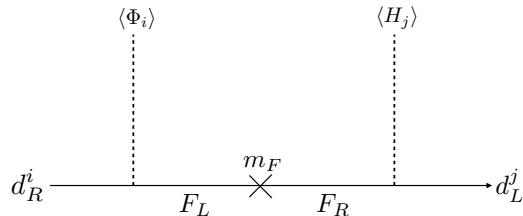


Figure 8: Rough sketch of another idea to generate the flavor violation.

main annihilation processes are the annihilations to the weak gauge bosons. This kind of DM scenario has been studied well based on the recent experimental results [53–57]. In this scenario, the mass differences of the scalars depend on the couplings, λ_4 and λ_5 . We find that less than $\mathcal{O}(10)$ GeV mass differences among the scalars of H_D can achieve the correct relic density in the DM mass region given by Eq. (36) [57]. The cross section for the spin-independent direct detection is estimated as Eq. (37), so the H_D DM could also be tested in the XENON1T experiment.

5 Summary and Discussion

The flavor structure in our nature is one of mysteries, that may be revealed by the Beyond Standard Model. We do not know why the fermion masses are so hierarchical and the quark mixing is very small. In the SM model, the flavor violating processes are described by the CKM matrix in the W boson interaction, and this description is consistent with the experimental results. The CKM matrix is very close to an identity matrix, but has small off-diagonal elements. This corresponds to the different mass bases of up-type quarks and of down-type quarks, so that this fact may imply the existence of new particles that interact with either up-type quarks or down-type quarks.

In this paper, we propose the possibility that the flavor symmetry breaks down in the hidden sector existing around $\mathcal{O}(1)$ TeV– $\mathcal{O}(10)$ TeV, and some extra particles mediate the flavor violating effect to the SM quark sector. Among the mediators, we can find DM candidates as well. The CKM mixing is radiatively generated, so that the CKM matrix directly relates to the structure of the mediation sector: the couplings with quarks and the masses of the mediators. We simply assume that the DM contribution to the CKM matrix is dominant, because DM is expected to be the lightest particle among the mediators. Then, we derive the connection among the CKM matrix, the flavor physics

and the DM physics. Interestingly, the constraints from the vacuum stability, the flavor physics and the DM relic density require that the DM mass is between $\mathcal{O}(1)$ TeV and $\mathcal{O}(10)$ TeV, and the spin-independent DM scattering cross section is close to the expected region of the XENON1T experiment. We find the significant deviations in the flavor physics, so that we can test our scenario in the future experiments of the flavor physics as well.

Our main motivations are to find the connection between DM and the quark mixing in the SM and to look for universal predictions of this kind of model that the CKM matrix is originated from the radiative corrections involving DM. Therefore, we have not constructed any explicit model for the hidden sector in this work, and concentrate on the light-scalar contributions in the simple assumption. Our results could be applied to many concrete models that radiatively induce the quark mixing and realize a DM candidate. The model-dependent analysis is, however, important to understand how large the parameter region covered by our study is. For instance, the flavor physics has been studied in the minimal supersymmetric model, where the quark mass matrix is radiatively induced [20]. In the model, the one-loop diagrams involving the superpartners of gluon and quarks lead the quark mixing and the mass hierarchy. Compared with our setup in Eq. (11), the bare coupling, y_d^i , has only one non-vanishing element and flavor U(2) symmetry is assigned in Ref. [20]. In this case, the bound from the $K_0 - \overline{K}_0$ mixing could be relaxed, if we assume that approximately only one U(2) breaking term, namely A-term, defines the mass eigenstates of the strange and down quarks. Then, one does not need large radiative contribution to realize the Cabibbo angle. In our setup, on the other hand, all mass eigenstates are given by the linear combinations of the bare couplings and the radiative corrections and the Cabibbo angle is generated by the radiative correction. Therefore, the bounds from the $K_0 - \overline{K}_0$ mixing and the EDM, that are only relevant to the radiative corrections, cannot be evaded. ¶ In addition, we suggest that the constraint on the CP-phase is the most stringent when the mass matrix is approximately in the form of Eq. (11). The study of the model with different forms from Eq. (11) will be given in future [58].

Let us also discuss the other scenarios, motivated by the origin of the CKM matrix. We did not qualitatively take into account the physics of $\phi_{1,2}$, $H'_{1,2}$ and the fields to break the flavor symmetry. There is a possibility that tree-level diagrams, as in Fig. 8, realize the quark mixing. In this case, some of the scalars such as $\phi_{1,2}$ develop the non-vanishing VEVs and the tree-level diagram simply generates the realistic down-type Yukawa couplings. This kind of model is much simpler and has been discussed, for instance, in the framework of the grand unified theory [3–6, 9, 59, 60]. In particular, the authors of Refs. [59, 60] recently consider such a simple setup for the realistic Yukawa couplings in the SO(10) grand unified theory, and study the FCNCs predicted by the fermion mass hierarchies and the quark mixing. In this case, however, scalar DM candidates, X and H_D , may decay to quarks because of the non-vanishing VEVs of $\phi_{1,2}$, so that we may have to introduce some additional particles to realize a DM candidate. Besides, there

¶We can also find the strong bound from the $K_0 - \overline{K}_0$ mixing in the supersymmetric model [15, 18].

are tree-level FCNCs suppressed by the masses of the extra colored particles. In this scenario, the predicted mass matrix of down-type quarks is in the same form introduced in Eq. (8), so that we could also apply our analysis to this new scenario. Including this type of diagram in Fig. 8, we will summarize possible setups motivated by both DM and the origin of the CKM matrix, and then discuss the universal predictions, the differences and relevant physics of each model [58].

Acknowledgments

We would like to thank Alejandro Ibarra for discussions and suggestions. S.O. is also grateful to the hospitality of Physik-Department T30d, Technische Universität München where the first stage of this work was done. The work of Y. O. is supported by Grant-in-Aid for Scientific research from the Ministry of Education, Science, Sports, and Culture (MEXT), Japan, No. 17H05404.

References

- [1] G. Hinshaw *et al.* [WMAP Collaboration], *Astrophys. J. Suppl.* **208**:19 (2013) [arXiv:1212.5226 [astro-ph.CO]].
- [2] P. A. R. Ade *et al.* [Planck Collaboration], *Astron. Astrophys.* **594**, A13 (2016) [arXiv:1502.01589 [astro-ph.CO]].
- [3] R. Barbieri and D. V. Nanopoulos, *Phys. Lett.* **91B**, 369 (1980).
- [4] R. Barbieri and D. V. Nanopoulos, *Phys. Lett.* **95B**, 43 (1980).
- [5] R. Barbieri, D. V. Nanopoulos and D. Wyler, *Phys. Lett.* **103B**, 433 (1981).
- [6] R. Barbieri, D. V. Nanopoulos and A. Masiero, *Phys. Lett.* **104B**, 194 (1981).
- [7] G. Kramer and I. Montvay, *Z. Phys. C* **11**, 159 (1981).
- [8] B. S. Balakrishna, *Phys. Rev. Lett.* **60**, 1602 (1988).
- [9] B. S. Balakrishna, A. L. Kagan and R. N. Mohapatra, *Phys. Lett. B* **205**, 345 (1988).
- [10] A. B. Lahanas and D. Wyler, *Phys. Lett.* **122B**, 258 (1983).
- [11] A. Masiero, D. V. Nanopoulos and K. Tamvakis, *Phys. Lett.* **126B**, 337 (1983).
- [12] S. M. Barr, *Phys. Rev. D* **31**, 2979 (1985).
- [13] A. L. Kagan, *Phys. Rev. D* **40**, 173 (1989).

- [14] M. Baumgart, D. Stolarski and T. Zorawski, Phys. Rev. D **90**, no. 5, 055001 (2014) [arXiv:1403.6118 [hep-ph]].
- [15] W. Altmannshofer, C. Frugiuele and R. Harnik, JHEP **1412**, 180 (2014) [arXiv:1409.2522 [hep-ph]].
- [16] F. Borzumati, G. R. Farrar, N. Polonsky and S. D. Thomas, Nucl. Phys. B **555**, 53 (1999) [hep-ph/9902443].
- [17] J. Ferrandis, Phys. Rev. D **70**, 055002 (2004) [hep-ph/0404068].
- [18] J. Ferrandis and N. Haba, Phys. Rev. D **70**, 055003 (2004) [hep-ph/0404077].
- [19] A. Crivellin, J. Girrbach and U. Nierste, Phys. Rev. D **83**, 055009 (2011) [arXiv:1010.4485 [hep-ph]].
- [20] A. Crivellin, L. Hofer, U. Nierste and D. Scherer, Phys. Rev. D **84**, 035030 (2011) [arXiv:1105.2818 [hep-ph]].
- [21] A. Thalapillil and S. Thomas, arXiv:1411.7362 [hep-ph].
- [22] X. G. He, R. R. Volkas and D. D. Wu, Phys. Rev. D **41**, 1630 (1990).
- [23] E. Ma, Phys. Rev. Lett. **112**, 091801 (2014) [arXiv:1311.3213 [hep-ph]].
- [24] E. Ma, Phys. Lett. B **741**, 202 (2015) [arXiv:1411.6679 [hep-ph]].
- [25] T. Nomura and H. Okada, Phys. Lett. B **761**, 190 (2016) [arXiv:1606.09055 [hep-ph]].
- [26] A. Natale, Nucl. Phys. B **914**, 201 (2017) [arXiv:1608.06999 [hep-ph]].
- [27] C. Kownacki and E. Ma, Phys. Lett. B **760**, 59 (2016) [arXiv:1604.01148 [hep-ph]].
- [28] A. E. Cárcamo Hernández, S. Kovalenko and I. Schmidt, arXiv:1611.09797 [hep-ph].
- [29] E. Aprile *et al.* [XENON Collaboration], JCAP **1604**, no. 04, 027 (2016) [arXiv:1512.07501 [physics.ins-det]].
- [30] C. Patrignani *et al.* [Particle Data Group], Chin. Phys. C **40**, no. 10, 100001 (2016).
- [31] CKMfitter global fit results as of Summer 2016 (ICHEP 2016 conference)
http://ckmfitter.in2p3.fr/www/html/ckm_main.html
- [32] K. G. Chetyrkin, J. H. Kuhn and M. Steinhauser, Comput. Phys. Commun. **133**, 43 (2000) [hep-ph/0004189].
- [33] H. Arason, D. J. Castano, B. Keszthelyi, S. Mikaelian, E. J. Piard, P. Ramond and B. D. Wright, Phys. Rev. D **46**, 3945 (1992).

- [34] T. Abe, J. Kawamura, S. Okawa and Y. Omura, JHEP **1703**, 058 (2017) [arXiv:1612.01643 [hep-ph]].
- [35] Jack Laiho, E. Lunghi and Ruth S. Van de Water, Phys. Rev. D **81**, 034503 (2010) [arXiv:0910.2928 [hep-ph]].
- [36] S. Aoki *et al.*, Eur. Phys. J. C **77**, no. 2, 112 (2017) [arXiv:1607.00299 [hep-lat]].
- [37] J. Brod and M. Gorbahn, Phys. Rev. Lett. **108**, 121801 (2012) [arXiv:1108.2036 [hep-ph]].
- [38] A. J. Buras, M. Jamin and P. H. Weisz, Nucl. Phys. B **347**, 491 (1990).
- [39] J. Brod and M. Gorbahn, Phys. Rev. D **82**, 094026 (2010) [arXiv:1007.0684 [hep-ph]].
- [40] G. Buchalla and A. J. Buras, Nucl. Phys. B **548**, 309 (1999) [hep-ph/9901288].
- [41] V. Lubicz and C. Tarantino, Nuovo Cim. B **123**, 674 (2008) [arXiv:0807.4605 [hep-lat]].
- [42] J. M. Pendlebury *et al.*, Phys. Rev. D **92**, no. 9, 092003 (2015) [arXiv:1509.04411 [hep-ex]].
- [43] Y. Amhis *et al.* [Heavy Flavor Averaging Group (HFAG)], arXiv:1412.7515 [hep-ex].
- [44] J. Hisano, J. Y. Lee, N. Nagata and Y. Shimizu, Phys. Rev. D **85**, 114044 (2012) [arXiv:1204.2653 [hep-ph]].
- [45] K. Fuyuto, J. Hisano and N. Nagata, Phys. Rev. D **87**, no. 5, 054018 (2013) [arXiv:1211.5228 [hep-ph]].
- [46] M. Jung and A. Pich, JHEP **1404**, 076 (2014) [arXiv:1308.6283 [hep-ph]].
- [47] B. Graner, Y. Chen, E. G. Lindahl, B. R. Heckel, Phys. Rev. Lett. **116**, 161601 (2016) [arXiv:1601.04339 [Atomic Physics]].
- [48] M. Escudero, A. Berlin, D. Hooper and M. X. Lin, JCAP **1612**, 029 (2016) [arXiv:1609.09079 [hep-ph]].
- [49] K. Griest and M. Kamionkowski, Phys. Rev. Lett. **64**, 615 (1990).
- [50] D. S. Akerib *et al.* [LUX Collaboration], Phys. Rev. Lett. **116**, no. 16, 161301 (2016) [arXiv:1512.03506 [astro-ph.CO]].
- [51] D. S. Akerib *et al.*, arXiv:1608.07648 [astro-ph.CO].
- [52] A. Tan *et al.* [PandaX-II Collaboration], Phys. Rev. Lett. **117**, no. 12, 121303 (2016) [arXiv:1607.07400 [hep-ex]].

- [53] A. Arhrib, Y. L. S. Tsai, Q. Yuan and T. C. Yuan, JCAP **1406**, 030 (2014) [arXiv:1310.0358 [hep-ph]].
- [54] A. Goudelis, B. Herrmann and O. Stal, JHEP **1309**, 106 (2013) [arXiv:1303.3010 [hep-ph]].
- [55] A. Ilnicka, M. Krawczyk and T. Robens, Phys. Rev. D **93**, no. 5, 055026 (2016) [arXiv:1508.01671 [hep-ph]].
- [56] M. A. Díaz, B. Koch and S. Urrutia-Quiroga, Adv. High Energy Phys. **2016**, 8278375 (2016) [arXiv:1511.04429 [hep-ph]].
- [57] A. Belyaev, G. Cacciapaglia, I. P. Ivanov, F. Rojas and M. Thomas, arXiv:1612.00511 [hep-ph].
- [58] Work in preparation.
- [59] J. Hisano, Y. Muramatsu, Y. Omura and M. Yamanaka, Phys. Lett. B **744**, 395 (2015) [arXiv:1503.06156 [hep-ph]].
- [60] J. Hisano, Y. Muramatsu, Y. Omura and Y. Shigekami, JHEP **1611**, 018 (2016) [arXiv:1607.05437 [hep-ph]].